

Narrowband, polarization insensitive all-fiber acousto-optic tunable bandpass filter

Kwang Jo Lee^{1*}, Dong Il Yeom², and Byoung Yoon Kim¹

¹Department of Physics, Korea Advanced Institute of Science and Technology (KAIST)
373-1 Guseong-dong, Yuseong-gu, Daejeon, 305-701, Korea

²Centre for Ultra-high bandwidth Devices for Optical Systems (CUDOS), School of Physics A28, University of
Sydney, NSW 2006 Australia

* kjl@kaist.ac.kr

<http://fiber.kaist.ac.kr>

Abstract: We demonstrate an all-fiber acousto-optic tunable bandpass filter exhibiting narrow optical bandwidth and negligible polarization dependence by employing a novel ultraviolet (UV)-induced core-mode blocker written in a high numerical aperture (NA) fiber. It was demonstrated that the device had the measured 3-dB optical bandwidth of 0.65 nm, the polarization-dependent center-wavelength splitting of 0.05 nm and the extinction ratio of -22dB at the wavelength around 1550 nm. The details of the transmission characteristics and the loss mechanism of the core-mode blocking element inscribed in the high NA fiber are discussed.

©2007 Optical Society of America

OCIS codes: (060.2310) Fiber optics; (230.1040) Acousto-optical devices

References and links

1. H. S. Kim, S. H. Yun, I. K. Hwang, and B. Y. Kim, "All-fiber acousto-optic tunable notch filter with electronically controllable spectral profile," *Opt. Lett.* **22**, 1476 (1997).
2. H. S. Park, K. Y. Song, S. H. Yun, and B. Y. Kim, "All-fiber wavelength-tunable acoustooptic switches based on intermodal coupling in fibers," *J. Lightwave. Technol.* **20**, 1864 (2002).
3. S. H. Yun and H. S. Kim, "Resonance in fiber-based acoustooptic devices via acoustic radiation to air," *IEEE Photon. Technol. Lett.* **16**, 147 (2004).
4. M. S. Lee, I. K. Hwang, and B. Y. Kim, "Acousto-optic tunable bandpass Filter," in *Proceedings of IEEE OptoElectronics and Communications Conference, WG Fibre Devices* (OECC/IOOC, Sydney, Australia, 2001), pp. 324-325.
5. D. A. Satorius, T. E. Dimmick, and G. L. Burdge, "Double-pass acoustooptic tunable bandpass filter with zero frequency shift and reduced polarization sensitivity," *IEEE Photon. Technol. Lett.* **14**, 1324 (2002).
6. P. Z. Dashti, C. -S. Kim, Q. Li, and H. P. Lee, "Demonstration of a Novel All-Fiber Bandpass Acousto-Optic Tunable Filter," in *Optical Fiber Communication Conference and Exposition and The National Fiber Optic Engineers Conference*, Technical Digest (CD) (Optical Society of America, 2005), paper OFC2. <http://www.opticsinfobase.org/abstract.cfm?URI=OFC-2005-OFC2>
7. K. J. Lee, D. I. Yeom, and B. Y. Kim, "Narrow-bandwidth acousto-optic tunable bandpass filter using dispersion compensating fiber," in *Proceedings of IEEE Pacific Rim Conference on Lasers and Electro-Optics* (Toshi Center Kaikan, Tokyo, Japan, 2005), pp. 1082-1083.
8. D. I. Yeom, H. S. Kim, M. S. Kang, H. S. Park, and B. Y. Kim, "Narrow-bandwidth all-fiber acoustooptic tunable filter with low polarization sensitivity," *IEEE Photon. Technol. Lett.* **17**, 2646 (2005).
9. Y. G. Han, S. H. Kim, S. B. Lee, U. C. Paek, and Y. Chung, "Development of a novel core mode blocker with H₂-loaded Ge-B co-doped fibers," *Electron. Lett.* **39**, 1107 (2003).
10. D. S. Starodubov, V. Grubsky, and J. Feinberg, "All-fiber bandpass filter with adjustable transmission using cladding-mode coupling," *IEEE Photon. Technol. Lett.* **10**, 1590 (1998).
11. J. -L. Archambault, L. Reekie and P. St. J. Russell, "100% reflectivity Bragg reflectors produced in optical fibres by single excimer laser pulses," *Electron. Lett.* **29**, 453 (1993).
12. P. St. J. Russell, J. -L. Archambault, and L. Reekie, "Fibre gratings," *Physics World*, **10**, 41 (1993).
13. K. O. Hill, B. Malo, F. Bilodeau, and D. C. Johnson, "Photosensitivity in optical fibers," *Annu. Rev. Mater. Sci.* **23**, 125 (1993).
14. M. Janos, J. Canning, and M. G. Sceats, "Incoherent scattering losses in optical fiber Bragg gratings," *Opt. Lett.* **21**, 1827 (1996).

15. H. Renner, D. Johlen, and E. Brinkmeyer "Modal field deformation and transition losses in UV side-written optical fibers," *Appl. Opt.* **39**, 933 (2000).
16. C. G. Askins and M. A. Putnam, "Photodarkening and photobleaching in fiber optic Bragg gratings," *J. Lightwave Technol.* **15**, 1363 (1997).

1. Introduction

Tunable bandpass filters are key components in optical communication networks and optical sensor systems. In particular, all-fiber acousto-optic tunable filters (AOTFs) have attracted considerable interest because of their advantages such as wide and fast wavelength tuning and variable attenuation with simple electric control [1, 2]. Practical notch filters with a simple AOTF structure have been realized based on wavelength selective acousto-optic coupling from the core mode to the cladding modes that can be easily removed [3]. In addition to the notch filters, bandpass filters are desired to expand the applications of such filters. Some key features required for a practical acousto-optic tunable bandpass filter (AOTBF) include availability of narrow linewidth, negligible polarization dependence, low loss, small form factor, high extinction ratio, environmental stability, and in some cases, no frequency shift. Several different AOTBFs have been demonstrated using core mode blockers with compact size [4, 5], and narrow bandwidth using high dispersion fiber and Sagnac interferometer [6]. However, a device having all of the desired properties has not been reported to our knowledge.

In this paper, we demonstrate an AOTBF that satisfies all of the desired properties mentioned above having narrow bandwidth (0.65 nm), low polarization dependent loss (0.18dB), low insertion loss (1dB), small form factor, and zero frequency shift. These properties were made possible by using a newly developed ultraviolet (UV)-induced core-mode blocker and a dispersion compensating fiber (DCF) [7]. The new core-mode blocker provides high extinction ratio with low transmission loss and negligible polarization dependence. The narrow bandwidth results from highly dispersive core mode, and the polarization insensitivity comes from the reduced thermal stress effect caused by the small core and depressed cladding structure [8].

2. Experiment and analysis

Figure 1 shows the schematic of an AOTBF. The AOTBF is composed of an acoustic transducer and a core-mode blocker in the middle section of the fiber. In the filter, the incident LP_{01} core mode is converted to the LP_{11} cladding mode at resonant wavelength by a flexural acoustic wave. The converted cladding mode passes through the core-mode blocker with small transmission loss and is coupled back to the core mode by the acoustic wave. On the other hand, the uncoupled core mode at non-resonance wavelengths suffers large loss by the core mode blocker. As a result, the device performs a bandpass filter function at a specific wavelength [4, 7]. The resonant wavelength and the transmitted power of the filter can be tuned by adjusting the frequency and the voltage of the applied electric signal, respectively.

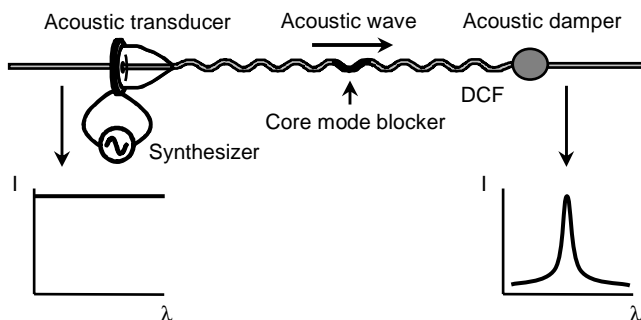


Fig. 1. Schematic of an acousto-optic tunable bandpass filter.

Some key performance parameters, such as insertion loss and extinction ratio, of the AOTBF is determined by how well the core-mode blocker eliminates the core mode without

inducing significant loss in the cladding mode. Novel fabrication methods of the core mode blocker for application to the long period fiber grating (LPFG) based all-fiber bandpass filters by exposing hydrogen-loaded optical fibers to local electric arc discharge [9] or near-UV light (300 - 305 nm) from an Ar ion laser [10] were previously reported. In our experiment, the core-mode blocker was fabricated by side illumination of KrF laser ($\lambda = 248$ nm, pulse repetition frequency of 1 to 10 Hz) with the energy of 280 mJ/pulse onto the hydrogen-loaded high numerical aperture (NA) fiber, because UV light of 248 nm spectral region could be more efficiently absorbed into the highly Ge-doped core of the fiber due to photosensitivity [13]. Figure 2 shows a damage track at the core-cladding boundary of the fiber section induced by UV radiation as in the case of fiber Bragg gratings [11]. The damage track is believed to be caused by the intense local heating due to interaction of the UV pulse with free-electron plasma [12]. The fabricated core-mode blocker was about 18-mm long, and the resultant core-mode loss was between 15dB and 30 dB over a broad wavelength range of 1200 to 1700 nm, as shown in Fig. 3.

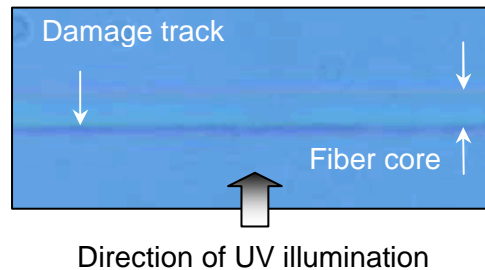


Fig. 2. Microscopic image of the damage track at the core-cladding boundary of the UV-exposed DCF.

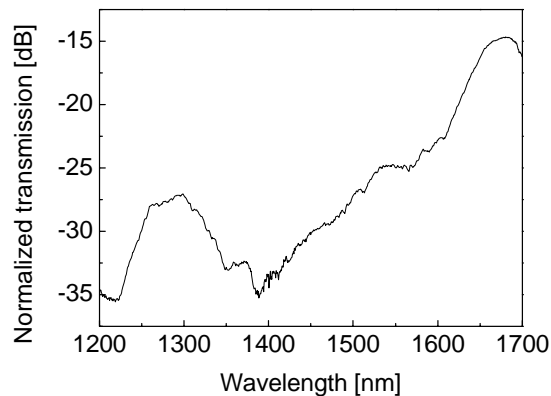


Fig. 3. Core mode loss of the fabricated core mode blocker.

Figure 4 shows the spectral characteristic of the fabricated core-mode blocker in the wavelength range of our current interest. It is interesting to note that the core-mode loss shows polarization dependence depending on the polarization direction of the side-illuminated UV light. When the polarization of the UV light beam is oriented parallel to the longitudinal axis of the fiber, no polarization dependence in transmission is observed within the measurement accuracy [Fig. 4(a)]. On the other hand, when the UV light whose polarization direction is perpendicular to the fiber axis is illuminated, the transmission exhibits strong polarization dependence [Fig. 4(b)]. The polarization dependence is attributed to UV induced anisotropy of the damage track [13], which is expected to cause the polarization dependent light scattering.

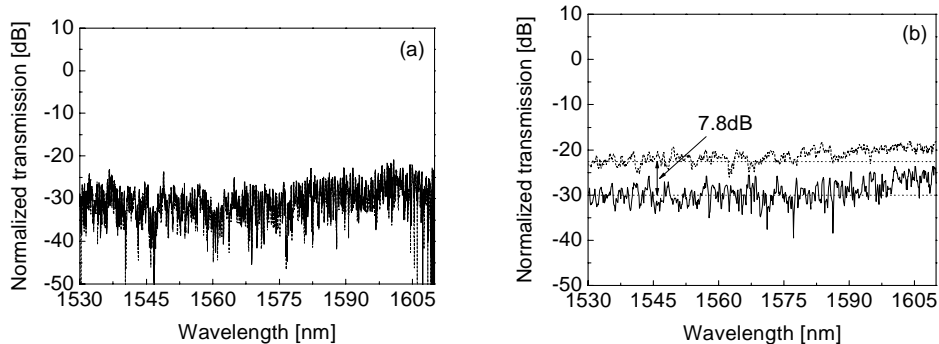


Fig. 4. The spectral characteristic of the fabricated core mode blocker irradiated from the side with (a) parallel and (b) perpendicularly polarized UV light to the longitudinal axis of the DCF.

In order to understand the loss mechanism in the core mode blocker, we measured the optical power scattered out of the fiber, coupled into the cladding modes, and back reflection. Figure 5 shows the experimental arrangement used to measure the scattered light radiating into the air. A high-sensitivity detector with a $0.7 \text{ mm} \times 0.7 \text{ mm}$ aperture was placed at 0.7 mm from the fiber. The detector was mounted on a translation stage moving along the whole length of the blocker. Broadband amplified spontaneous emission from an Erbium doped fiber amplifier (EDFA) with the wavelength range of 1530 nm to 1610 nm was used as an incoherent and unpolarized light source. The measured power at the image point $P(Z, \Phi)$ of the moving detector due to the scattered power at the object points $p(z, \varphi)$ of the core mode blocker can be expressed as following convolution integral:

$$P(Z, \Phi) = \iint p(z, \varphi) \cdot G(Z - z, \Phi - \varphi) dz d\varphi \quad (1)$$

where $G(Z - z, \Phi - \varphi)$ is the point spread function describing the two-dimensional aperture structure. The integration is carried out over the aperture width l in the direction of the fiber axis and the acceptance angle θ determined by the aperture dimension and a distance between the fiber and the aperture. If we assume the scattered power from the core mode blocker to be independent of object point coordinates, the Eq. (1) can be expressed as follows.

$$P(Z, \Phi) = \int_z^{Z+l} p(z) dz \cdot \int_{\Phi-\theta/2}^{\Phi+\theta/2} p(\varphi) d\varphi \quad (2)$$

Using the Eq. (2), the distribution of scattered power from the core mode blocker $p(z, \varphi)$ can be obtained as a function of the position (z) along the length of the blocker and the scattering angles (φ). The total power of the scattered light from the core mode blocker into the air is then determined by volume integral of the distribution of scattered power $p(z, \varphi)$ in cylindrical coordinates.

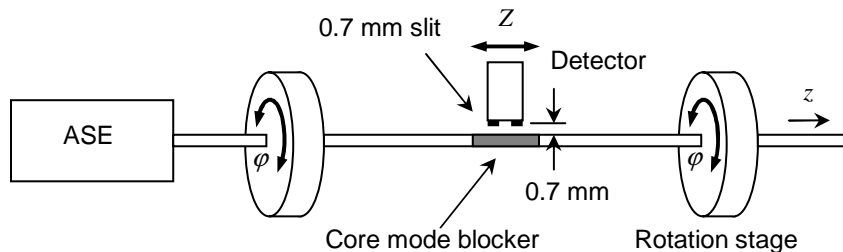


Fig. 5. Experimental configuration for measuring the power of side-scattered light from the core mode blocker. ASE, amplified spontaneous emission.

Figure 6 shows a polar plot of the scattered light from the core mode blocker at the maximum scattering point in the z direction. In this plot, the large arrow at the left indicates the direction of incident UV irradiation. We can see that the scattered light has a strong angular dependence that coincides with results reported for UV-processed optical fibers [14]. The total power scattered out of the fiber integrated over the whole blocker length and scattering angles reached about 90% of the launched power. Next, the optical power scattered into the cladding was measured as follows. First, the polymer jacket of the fiber between the blocker and the photodetector was removed and the total output power from the fiber end is measured. Then the fiber section between the blocker and the detector is immersed in the index matching oil to strip the cladding modes, and the output power was measured. The difference in the two power measurement corresponds to the power scattered into the cladding by the blocker, which was about 10% of the initially input power. Finally, the back reflection to core mode was measured to be -31.5dB ($< 0.1\%$) of the total input power. From these measurements, we could conclude that the main contributions of the core mode loss at the core mode blocker were scattering out of the fiber and transition losses into the cladding modes. UV-induced absorption, another possible reason to cause the core mode loss, has no remarkable effect on core mode loss in this case. Because the core mode blocker is composed of the physical damage track at the core-cladding boundary of the fiber, while UV-induced absorption at near-infrared (NIR) spectral region is mainly associated with UV-induced refractive index change [15, 16].

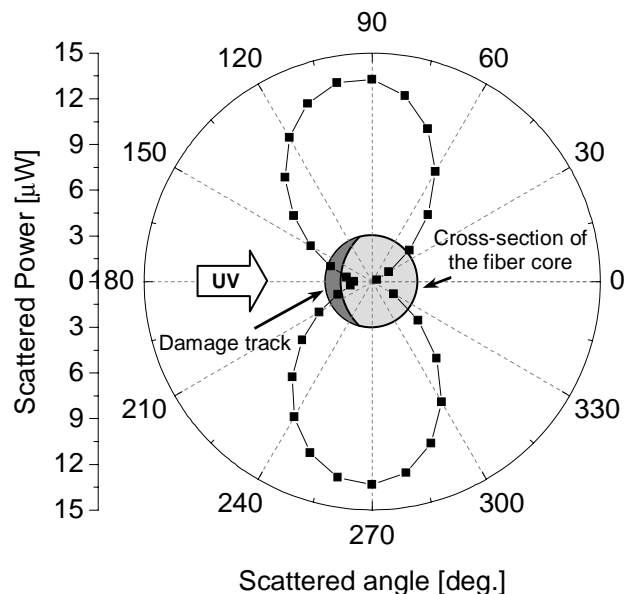


Fig. 6. Polar plot of scattered light from the core mode blocker. The large arrow at the left indicates the direction of incident UV irradiation.

We built an AOTBF using a DCF (-95 ps/nm/km, core radius of $1\mu\text{m}$, index difference of 2% and depressed cladding structure) with a 20-cm-long interaction region, with a core mode blocker located at the center of the region. In order to reduce the polarization dependence of the transmission loss, the core mode blocker was fabricated by a UV light beam whose polarization direction was oriented parallel to the longitudinal axis of the fiber. Figure 7(a) shows the measured transmission spectrum of the filter at the acoustic frequency of 2.636 MHz. Optical transmission spectra for two orthogonal input polarizations were also shown in the inset of Fig. 7(a). The 3 dB bandwidth of 0.65 nm with the extinction ratio of 24.5 dB was achieved and the polarization-dependent center-wavelength splitting was < 0.05 nm at the wavelength around 1550 nm. The insertion loss of the device was less than 1 dB but the splice

loss between SMF and DCF was 2.4dB that could be reduced. Figure 7(b) shows the center wavelength of the AOTBF as a function of the acoustic frequency showing an almost linear relationship.

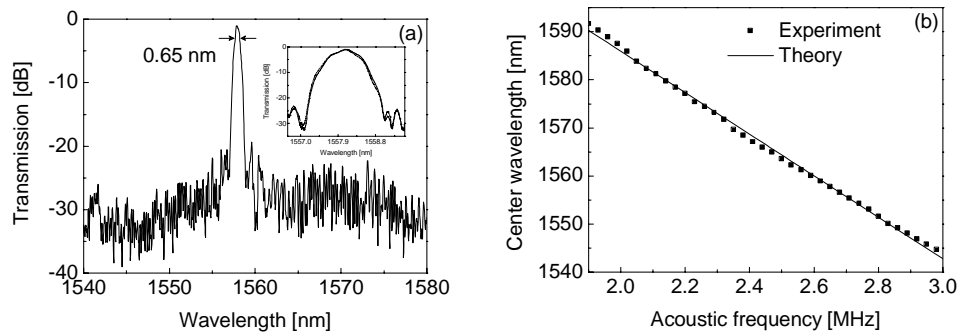


Fig. 7. (a). Measured transmission spectrum of the acousto-optic tunable bandpass filter for the acoustic frequency of 2.636 MHz and (b) Center wavelength of the acousto-optic tunable bandpass filter as a function of the acoustic frequency. The Inset shows optical transmission spectra for two orthogonal input polarizations.

3. Conclusion

In conclusion, we have demonstrated a novel all-fiber acousto-optic tunable bandpass filter using a high performance core-mode blocker written in high NA fiber. The filter had a narrow bandwidth (0.65 nm 3dB bandwidth), polarization insensitivity (0.05 nm) and high extinction (-22dB), low insertion loss (1dB) and small form factor. The transmission characteristics and the loss mechanism of the UV-induced core-mode blocker were investigated in detail.

Acknowledgments

The authors thank Dr. Hyuk-Jin Yoon of Korea Railroad Research Institute and Kyung Joon Han of Optical Engineering and Quantum Electronics Laboratory in Seoul National University for allowing the use of KrF eximer lasers.